

DISTRIBUTION OF KOLMOGOROV-SINAI ENTROPY IN SELF-CONSISTENT MODELS OF BARRED GALAXIES

H. WOZNIAK

IGRAP/Observatoire de Marseille, F-13248 Marseille cedex 4, France

E-mail: wozniak@observatoire.cnrs-mrs.fr

and

D. PFENNIGER

Observatoire de Genève, CH-1290 Sauverny, Switzerland,

E-mail: Daniel.Pfenniger@obs.unige.ch

Abstract. The properties of chaos in 2D self-consistent models of barred galaxies are investigated using Kolmogorov-Sinai entropy h_{KS} . These models are constructed with Schwarzschild's method which combines orbits as elementary building blocks.

Most models are dominated by chaos near the $2/3$ of the length of the bar and close to corotation. These locations correspond to regions where star-forming HII regions are observed because gas clouds could shock, shrink and fragment such that star formation could be ignited.

The model the most similar to N -body models shows a peak of h_{KS} between the corners of the rectangular-like x_1 orbits and the maximum extension points of the Lagrangian orbits. This emphasizes the role of Lagrangian orbits in the morphology of bars. Most models essentially contain 'semi-chaotic' orbits confined inside the corotation.

1. Introduction

The determination of the analytical distribution function of galaxies, in particular barred galaxies, remains a long standing problem. Freeman (1966) has been the first to propose an analytical formulation of the distribution function of a stellar bar with a model of an homogeneous triaxial ellipsoid for which the centrifugal and central forces are in equilibrium along the major-axis of the bar. This model has, however, unrealistic properties (e.g. the x -axis Lagrangian points extend over the whole major axis instead of being, as expected, located slightly beyond the end of the bar).

A numerical line of attack has been initiated by Schwarzschild (1979) to study triaxial elliptical galaxies. From a library of orbits in a triaxial mass model he determined numerically one of the all possible distribution functions reproducing the initial mass model.

With some improvements, Pfenniger (1984b; 1985) and Wozniak & Pfenniger (1996; 1997) used it to compute self-consistent models of barred galaxies. Apart from Zhao's study (1996) of the Milky Way bar, these studies remain the only attempts to apply Schwarzschild's method to fast rotating bars. These studies exploited more extensively the possibilities offered by Schwarzschild's technique. Instead of finding a single feasible kinematic model for a given mass model, the set of possible solutions was explored by looking at its extreme global properties



(energy, angular momentum, etc.) that a given mass distribution does allow while remaining self-consistent. The obtained distribution functions and linear superpositions of them are all possible self-consistent solutions satisfying the equilibrium condition. So the advantage of Schwarzschild's method over N -body models is that the whole solution set allowed by an arbitrary mass distribution can be explored, while its main drawback is that no stability information is provided. The stability of such models is best studied with a N -body code whose initial conditions of particles are drawn from a particular solution (cf. Zhao, 1996).

Chaotic motion is expected to form a significant part of the orbits populating stellar bars. However, because realistic galactic distribution functions are difficult to construct, the proportion of chaotic orbits is barely determined. Pfenniger (1984b) found between 10 and 30% of chaotic orbits in his models. In their N -body models, Sparke & Sellwood (1987) and Pfenniger & Friedli (1991) found a "hot" population which belong both to the bar and the stellar disc. The hot population may contribute up to 30% of the total mass. Kaufmann (1993) and Kaufmann & Contopoulos (1996) confirmed that between 5 and 14% of chaotic orbits populate the bar and as much belong to the "hot" population. However, chaotic orbits play a major role in the secular evolution of galaxies because they introduce irreversibility. A notion such as adiabatic invariance is based on the assumption that phase space is structured by isolating quasi-integrals, thus the absence of some of these means that much more freedom to morphology changes is left to slightly or slowly perturbed orbits. Thus, we decided to quantitatively determine the proportion of such orbits in Wozniak & Pfenniger's (1997) models of barred galaxies. The Kolmogorov-Sinai entropy was used as a tool to quantify the amount of orbital chaos in a stellar system by Udry & Pfenniger (1988).

We will describe Schwarzschild's technique used to built self-consistent models in Sect. 2, the properties of the models in Sect. 3, and how we compute the Kolmogorov-Sinai entropy in Sect. 4. In Sect. 5, we present our preliminary results. Finally, we give our conclusions and a few implications for the morphology of barred galaxies in the last section.

2. Schwarzschild's technique

In Schwarzschild's (1979) method, the configuration space is discretized into N_{cell} compact cells. Phase space is discretized by N_{orb} orbits that are computed in the gravitational potential generated by the chosen mass density. The fraction of time spent by each orbit in each cell (B_{ij}) is called the occupation. The mass M_i inside any cell i is thus a weighted sum of the B_{ij} . The N_{orb} weights X_j of the sum are the unknowns, and are constrained to be positive or zero (i.e. non-negative) to represent a physical mass. Equivalently, we can express this problem as a set of

N_{cell} linear equations with N_{orb} unknowns:

$$M_i = \sum_{j=1}^{N_{\text{orb}}} B_{ij} X_j \quad i = 1, \dots, N_{\text{cell}}, \quad (1)$$

$$X_j \geq 0, \quad j = 1, \dots, N_{\text{orb}}. \quad (2)$$

This is a linear programming problem (cf. Chvátal, 1983). Of course, with the positivity constraint the number of orbits N_{orb} must be larger than the number of cells N_{cell} to have any possibility to find at least one solution.

As in Pfenniger (1984b) and Wozniak & Pfenniger (1997), instead of the traditional Simplex algorithm of linear programming, we used the NNLS (Non Negative Least Squares) algorithm (Lawson & Hanson, 1974, 1995) which finds a positive least squares solution of Eq. (1). The advantage of NNLS over the Simplex algorithm is to provide, in case no exact solution does exist, the nearest approximate solution in the least-squares sense, instead of nothing for the Simplex. But when a solution set does exist, it finds *one of the exact solutions*, the one which minimizes $\|X\|$. The ability of NNLS to find exact solutions when they exist has been sometimes overlooked. Indeed, when the residuals vanish the solution found by NNLS is exact. For all basic solutions computed by Wozniak & Pfenniger (1997), the relative error on the mass as computed with Eq. (1) is of the order 10^{-7} , i.e., of the order of the round-off errors.

The minimization or maximization of basic solutions is obtained by adding a ‘cost’ function perturbing the set of equations (1) (see Pfenniger (see Pfenniger, 1984b for more details). The cost function, also called objective function, can be any linear function of the weights X_j . If Z_j represents a physical quantity then the objective function is:

$$\sum_{j=1}^{N_{\text{orb}}} Z_j X_j \quad (3)$$

normalized so that $\max(Z_j) = 1$ and $\min(Z_j) = 0$. For a given orbit j , Z_j can be the Jacobi constant E_{Jj} , the time-averaged z -angular momentum \overline{L}_{zj} , the absolute value of the time-averaged z -angular momentum $|\overline{L}_z|_j$, the energy $E_j = E_{Jj} + \Omega_p \overline{L}_{zj}$, where Ω_p is the rotation frequency of the bar pattern, or the Kolmogorov-Sinai entropy h_{KSj} . It can also be any linear relation between different of the above quantities. Since the domain of feasible solutions is convex (cf. Pfenniger, 1984b) Fig. 5), we need only to compute ‘extreme’ models that serve to delimit the domain. Hereafter, we call $\min(Z)$ or $\max(Z)$ models which respectively minimize or maximize the objective function Z . Intermediate models can always be constructed by a linear superposition of basic models, while the converse is false.

3. The self-consistent models

We reuse Wozniak & Pfenniger's (1997) self-consistent models to allow some comparisons. We have also computed two new models which are extremum of the Kolmogorov-Sinai entropy (cf. next section). These models share the following properties:

1. The mass model consists of a Miyamoto disk and a $n = 2$ Ferrers (1877) bar (cf. Pfenniger, 1984a for more details). This mass model is a first order approximation of the real mass distribution in barred galaxies.
2. Inside the corotation radius, the computational polar grid contains 24 cells in r , 20 in θ . The radial resolution is 4 cells per length unit, i.e. 250 pc. The central part ($r = 0$) of the grid consists of a single circular cell. We have used the symmetries of the mass density w.r.t. both axes to fold space onto the first quadrant.
3. The set of orbits which solves Eq. (1) belongs to a wide library of roughly 4000 orbits. Wozniak & Pfenniger (1997) carefully built this library keeping four properties under control: 1) the occupation of each individual orbit B_{ij} is time independent in order to ensure the construction of a model to a pre-determined level of time independence, 2) the library includes trapped orbits around stable periodic orbits as well as chaotic orbits, 3) identical occupation numbers B_{ij} for two orbits with distinct initial conditions imply that the B matrix is degenerate and the problem becomes "ill-posed". Redundant orbits have thus been removed, 4) aliases between the time steps, total time integration and the orbit natural frequencies are avoided.

The only difference between the models is the kind of objective function which is minimized or maximized. We have retained 6 models from Wozniak & Pfenniger (1997), namely the $\min(|\overline{L_z}|)$, $\max(|\overline{L_z}|)$, $\min(\overline{L_z})$, $\max(\overline{L_z})$, $\min(E_J)$ and $\min(E)$ models. Moreover, we have computed two new models ($\min(h_{KS})$ and $\max(h_{KS})$) described in the next section.

4. Computation of Kolmogorov-Sinai entropy

As we would like to measure the level of chaos of each models, we have computed the Lyapunov exponents for each orbits of the library. We globally followed the same rules as Udry & Pfenniger (1988): we integrate the equations of motion simultaneously with the variational equations. The two pairs $(\lambda_k, -\lambda_k)$ of Lyapunov exponents are computed with a Gram-Schmidt orthogonalization. For each orbit, the computations are performed until the fluctuations of the space density become lower than a given threshold (0.5%). This ensures that each orbit is close to be time independent. The most chaotic orbits do require longer integration times. In WP97, integration times range between $2T_{\text{bar}}$ for the regular orbits closest to the centre and $4500 T_{\text{bar}}$ for the most chaotic ones. Here, we have computed orbits during at least $T_{\text{min}} = 18 T_{\text{bar}}$. We thus name 'regular' orbits with $h_{KS} < \log(T_{\text{min}})/T_{\text{min}} \approx 0.0038$.

Such long calculation times are justified on the ground that the exercise here is to mimic analytical models, which if integrable would correspond to an infinite integration time. Therefore the maximum retained integration time has been deliberately chosen, when necessary, much larger than a typical galaxy physical age.

The Kolmogorov-Sinai entropy h_{KS} of an orbit can be viewed as the rate at which it loses information about its initial conditions. This quantity has been shown by Pesin (1977) to be equal to the sum of the positive Lyapunov exponents. For a given orbit j , a proper measure of this loss (or gain depending on the viewpoint) of information is:

$$h_{KS_j} = \sum_{\lambda_{k_j} > 0, k=1}^4 \lambda_{k_j}. \quad (4)$$

In Hamiltonian systems the entropy h_{KS_j} vanishes only for regular orbits. Orbits with non-zero h_{KS_j} have a sensitive dependence on initial conditions which is a possible criterion of chaos.

For the computation of the solutions for the $\min(h_{KS})$ and $\max(h_{KS})$ models, the objective function is:

$$h_{KS} = \sum_{j=1}^{N_{orb}} h_{KS_j} X_j \quad (5)$$

where h_{KS} is the Kolmogorov-Sinai entropy of the whole system.

The spatial distribution of Kolmogorov-Sinai entropy (h_{KS_i}) is obtained with:

$$h_{KS_i} = \frac{1}{M_i} \cdot \sum_{j=1}^{N_{orb}} h_{KS_j} B_{ij} X_j \quad (6)$$

for each cell i .

5. Results

Figs. 1 and 2 show the spatial distribution of h_{KS} . Regions with $h_{KS} < 0.0038$ ('regular' orbits) are restricted to the inner part of the bar and to the minor-axis ($3 \lesssim x \lesssim 4$). The nucleus is always a global minimum because in this model near the centre the potential is nearly harmonic, i.e., integrable. This does not mean that 'regular' orbits are excluded from the other regions of the model but their contribution is negligible w.r.t. non-regular orbits.

The contribution of chaotic orbits leads to maxima in the h_{KS} distribution in essentially two regions:

1. Along the corotation radius, especially near the $L_{1,2}$ Lagrangian points. Pfenniger (1984b) and Kaufmann & Contopoulos (1996) already claimed that chaotic orbits contribute essentially to the mass near $L_{1,2}$ points. Our study confirm this behavior.

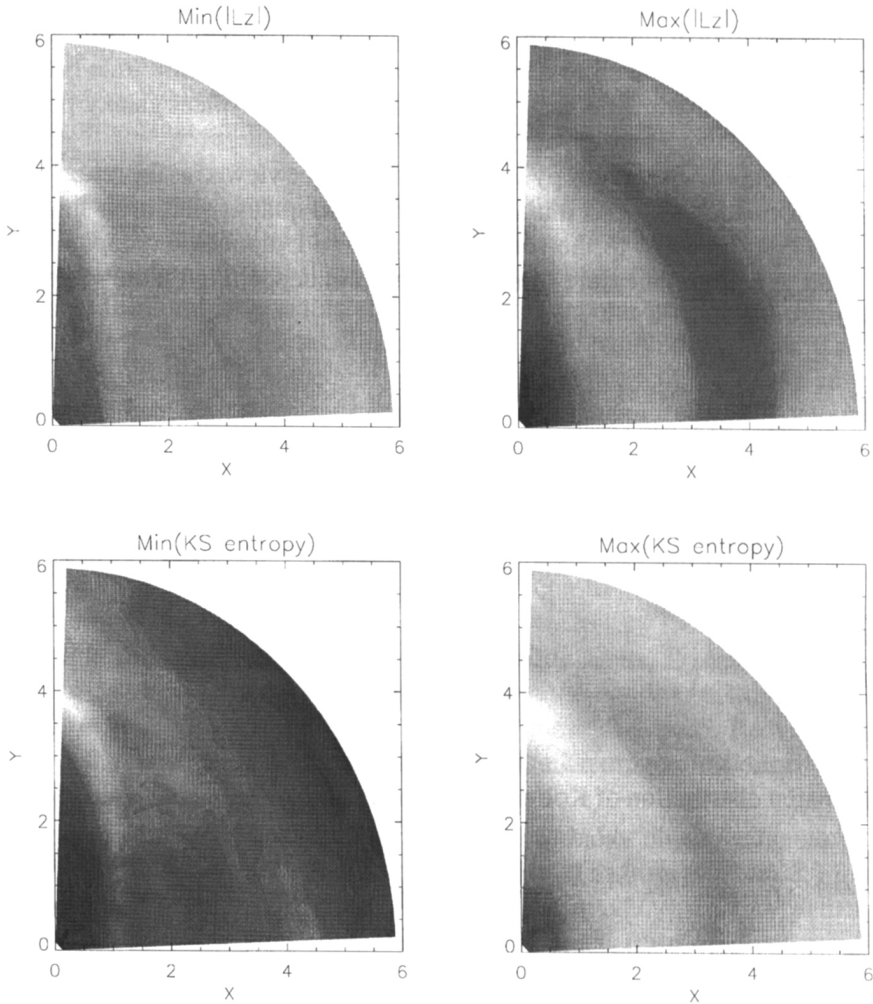


Fig. 1. Spatial KS entropy distribution h_{KS} , for the first quadrant of our mass model. Models $\min(E_J)$, $\min(E)$, $\min(\overline{L_z})$ and $\max(\overline{L_z})$ are displayed. The stellar bar (6 kpc long) is aligned with the y -axis. The highest values of h_{KS} , are white, the lowest are black

2. Along the major-axis of the bar ($3.5 \lesssim y \lesssim 4$), at the apocentre of the more elongated elliptical-like x_1 orbits. Indeed, the mass density response of an orbit trapped around the x_1 family is maximum at this location (cf. Fig. 3). Thus, most of the mass in this region is due to x_1 -trapped orbits.

The most chaotic models are the $\min(\overline{L_z})$, $\min(|\overline{L_z}|)$ and, obviously $\max(h_{KS})$ models. Wozniak & Pfenniger (1997) noted that the $\min(|\overline{L_z}|)$ model shows a similar distribution function than an N -body model by Pfenniger & Friedli (1991). The $\min(|\overline{L_z}|)$ model maximizes the contribution of orbits elongated along the bar. It favors the orbits trapped around the x_1 family at the expense of the hot population

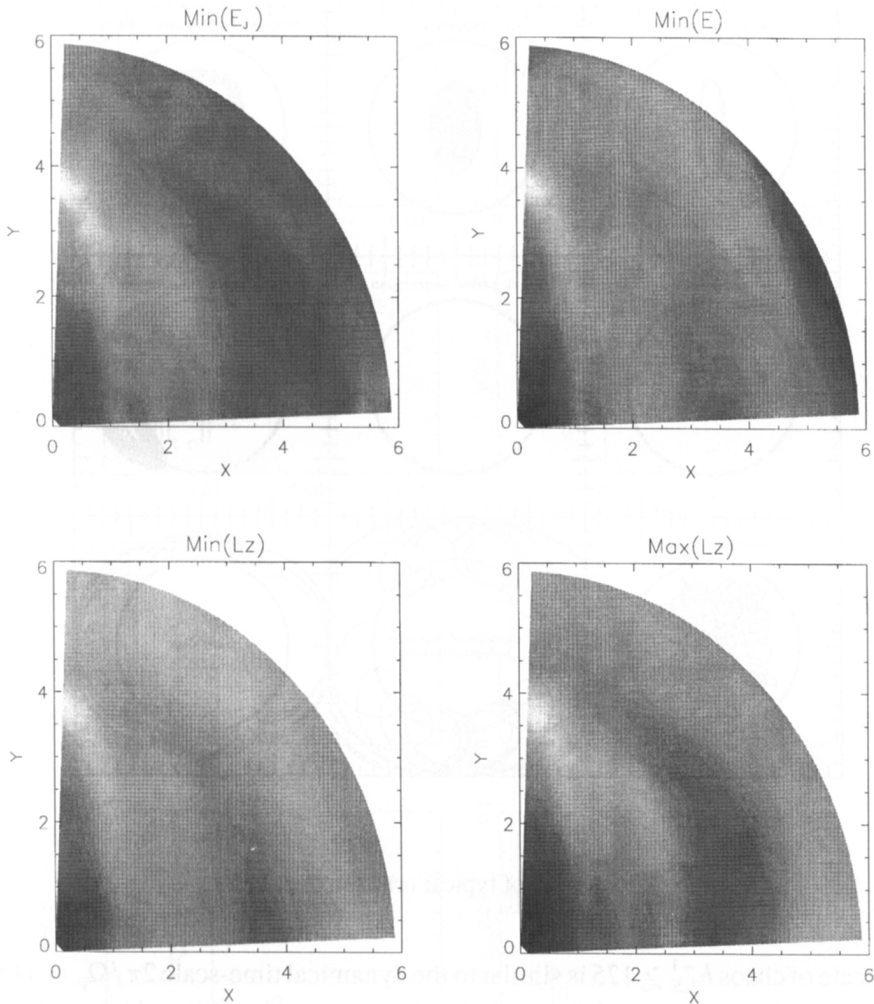


Fig. 2. As for Fig. 1, but for models $\min(|\overline{L_z}|)$, $\max(|\overline{L_z}|)$, $\min(h_{KS})$ and $\max(h_{KS})$

which populates mostly a region that includes the corotation. The maximum of h_{KS} located at $x \approx 2.6$, $y \approx 4.7$ is mostly due to rectangular-like x_1 -trapped orbits with Jacobi constants higher than the one at the ultra-harmonic 4/1 bifurcation. Moreover, the maximum extension of Lagrangian orbits which circulate around the $L_{4,5}$ Lagrangian points is close to this maximum of h_{KS} .

The less chaotic models are the $\min(E_J)$ and $\min(h_{KS})$ models. Pfenniger (1984b) already noted that the $\min(E_J)$ model has the simplest velocity field.

The mass distribution as a function of h_{KS} (Fig. 4) shows that most of the mass is due to orbits with $h_{KS} \lesssim 0.008$. This means that a single population of 'regular' orbits cannot account for the mass distribution. Non-regular orbits are thus unavoidable. For comparison, the frequency $\Omega_p = 0.0547$, which shows that the

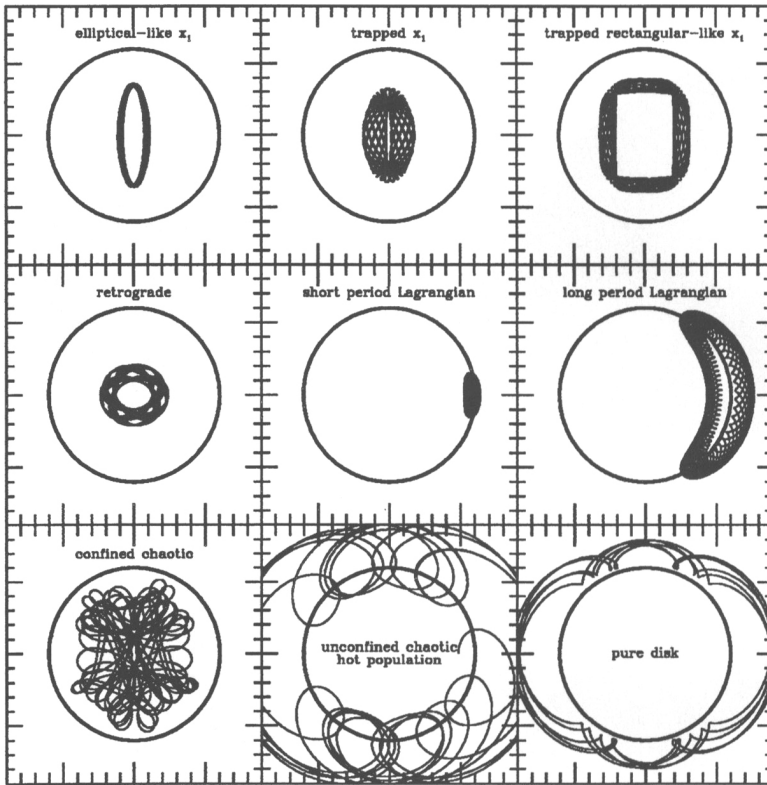


Fig. 3. Examples of typical orbits in the library

time-scale of chaos $h_{\text{KS}}^{-1} \gtrsim 125$ is similar to the dynamical time-scale $2\pi/\Omega_p \approx 115$.

One can also define another population in non-regular orbits which peaks at $h_{\text{KS}} \approx 0.01$. This component is clearly present in almost all models but $\min(E_J)$ and $\min(h_{\text{KS}})$. Orbits with $h_{\text{KS}} \gtrsim 0.013$ contribute less than a few percent to the total mass of the models. Globally, when chaotic orbits contribute to the mass density, they are only moderately chaotic orbits ($h_{\text{KS}} \lesssim 0.013$), even for the model that maximizes the Kolmogorov-Sinai entropy. These orbits remain confined inside the corotation (cf. Fig. 3). They are similar to the ‘semi-chaotic’ orbits of Wozniak (1994).

6. Astrophysical implications and conclusions

Most models are not only dominated by chaos close to corotation but also near the 2/3 of the length of the bar. This is of great importance for the gas flow along the bar. Indeed, this highly chaotic region should correspond to a region where the gas

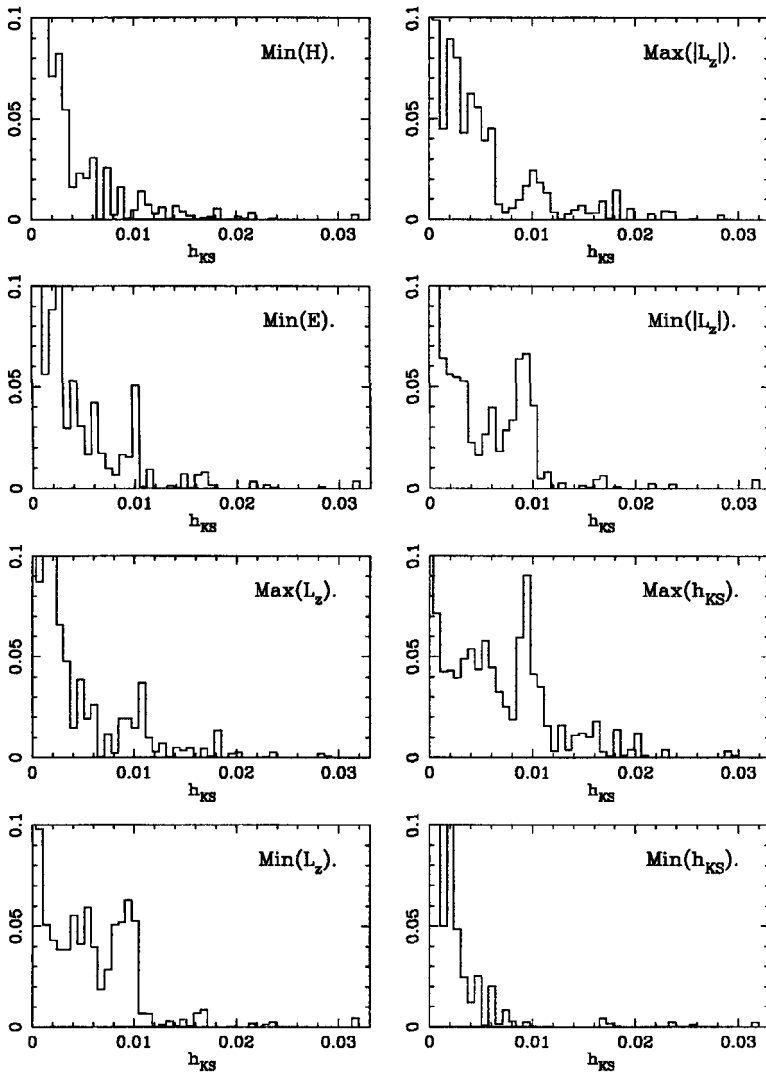


Fig. 4. Mass distribution (in fraction of mass inside the corotation radius) w.r.t. the KS entropy for the eight models

clouds could shock, shrink and fragment such that star formation could be ignited. In many barred galaxies one observes indeed HII regions located near the middle of the major-axis of the stellar bar.

The $\min(|\overline{L_z}|)$ model (the most similar to N -body models) shows a peak of h_{KS} , between the corners of the rectangular-like x_1 orbits and the maximum extension points of the Lagrangian orbits. This emphasizes the role of Lagrangian orbits in the morphology of bars. Moreover, although our mass model is not designed to study the spiral structure, it should be noted that the location of these maximums

roughly corresponds to the starting points of the spiral structure of strong barred galaxies.

All the models, even those with high total KS entropy (e.g. $\min(\overline{L_z})$ and $\max(h_{KS})$), essentially contain orbits with $h_{KS_j} < 0.013$ which are not extremely chaotic orbits. Indeed, these orbits remain confined inside the corotation. They are in fact *semi-chaotic* orbits. These orbits have the same nature that the ones which seem to be responsible for the rectangular-like shape of strong bars (Wozniak, 1991), (Wozniak, 1994).

Acknowledgements

All the computations were done on the IGRAP computer facilities. This work has been supported by the Swiss National Science Foundation. We thank the anonymous referee for constructive remarks.

References

- Chvátal V.: 1983, *Linear Programming*, Freeman, New York
- Ferrers N.M.: 1877, *Quart. J. Pure Appl. Math.* **14**, 1
- Freeman K.C.: 1966, *Mon. Not. R. Astr. Soc.* **134**, 1
- Kaufmann D.E.: 1993, Ph D. Thesis, Univ. of Florida
- Kaufmann D.E., Contopoulos G.: 1996, *A&A* **309**, 381
- Lawson C.L., Hanson R.J.: 1974, *Solving Least Squares Problems*, Prentice-Hall, Englewood Cliffs, New Jersey; 1995, *Classic in Applied Mathematics 15*, SIAM, Philadelphia (updated NNLS routines are available at <http://www.netlib.org>)
- Pesin Y.B.: 1977, *Russ. Math. Surveys* **32**, 55
- Pfenniger D.: 1984a, *A&A* **134**, 373
- Pfenniger D.: 1984b, *A&A* **141**, 171
- Pfenniger D.: 1985, Ph D Thesis, University of Geneva
- Pfenniger D., Friedli D.: 1991, *A&A* **252**, 75
- Schwarzschild M.: 1979, *ApJ* **232**, 236
- Sparke L., Sellwood J.A., 1987, *MNRAS* **225**, 653
- Udry S., Pfenniger D.: 1988, *A&A* **198**, 135
- Wozniak H.: 1991a, Ph.D. Thesis, University of Paris 7
- Wozniak H.: 1994, in *Ergodic Concepts in Stellar Dynamics*, Gurzadyan V.G. & Pfenniger D. (eds.), *Lecture Notes in Physics 430*, Springer-Verlag, Heidelberg, p. 264
- Wozniak H., Pfenniger D., 1996, in: *Barred Galaxies*, Buta R., Elmegreen B.G., Crocker D.A. (eds.), *Proc. IAU Coll 157, ASP Conferences Series*, p. 445
- Wozniak H., Pfenniger D.: 1997, *A&A* **317**, 14
- Zhao H.: 1996, *MNRAS*, **283**, 149